ФИЗИКА ЭЛЕМЕНТАРНЫХ ЧАСТИЦ И АТОМНОГО ЯДРА
2010. Т. 41. ВЫП. 6

SELF-CONSISTENT MEAN-FIELD DESCRIPTION OF NUCLEAR STRUCTURE AND DYNAMICS — A STATUS REPORT

J. Erler[1], *W. Kleinig*[2], *P. Klüpfel*[1], *I. Kvasil*[3], *V. O. Nesterenko*[2], *P.-G. Reinhard*[1]

[1]Institut für Theoretische Physik, Universität Erlangen, Erlangen, Germany
[2]Joint Institute for Nuclear Research, Dubna
[3]Institute of Particle and Nuclear Physics, Charles University, Praha

This contribution deals with the predictive power of the Skyrme–Hartree–Fock model. First, we discuss the phenomenological adjustment of the Skyrme energy-functional and the choice of proper fit data. Then, we check the reliability in extrapolations to other observables and nuclei, using two strategies: first, comparison with data for observables not included in the fit, and second, an estimate of the extrapolation error by virtue of the least-squares fitting techniques. Test cases will be energies of extremely neutron rich Sn isotopes as well as energies, giant resonances, and fission properties of superheavy elements.

PACS: 21.60.-n

INTRODUCTION

Experiments on exotic nuclei far off the valley of stability are making steady progress and provide an enormous amount of new experimental data on basic nuclear properties. This calls for further development of nuclear structure theory. We will here report briefly recent achievements in the Skyrme–Hartree–Fock (SHF) method, for recent developments see, e.g., [1–3] and for extensive reviews [4,5]. The SHF approach provides a reasonably motivated framework for a universal, effective energy functional but leaves a couple of free parameters which are to be adjusted phenomenologically. The two key problems are then: first, to sort out a proper choice of the data set used for the adjustment, and second, to estimate the reliability of the functional when extrapolating to new observables outside the fitting set. These will be addressed in the following. Section 1 gives a brief overview of SHF and fitting strategies. Section 2 discusses a few typical examples for extrapolations and scrutinizes their reliability.

1. BRIEF REVIEW OF SKYRME-HARTREE–FOCK METHOD

The starting point is the Skyrme–Hartree–Fock (SHF) energy functional which is summarized very compactly in Fig. 1. The interaction energy is modeled

in terms of the Skyrme energy density $\mathcal{E}_{\rm Skyrme}$ and the pairing energy density $\mathcal{E}_{\rm pair}$ which are simple functions of local densities and currents (we have dropped in Fig. 1 the time-odd terms for simplicity, full details are found in [4, 5]). The building principle for $\mathcal{E}_{\rm Skyrme}$ is obvious: pairwise couplings between the density ρ and all other densities or the gradient of density, augmented by one term carrying more involved density dependence ($\propto B_3, B_3'$), and repeated in similar form in the isovector channel. One can argue that this form is the natural outcome of any «low q expansion» of a microscopic effective two-body interaction [5]. The free parameters of the ansatz are summarized at the bottom of Fig. 1. They are grouped with respect to their importance. This grouping will become clear in the next paragraph.

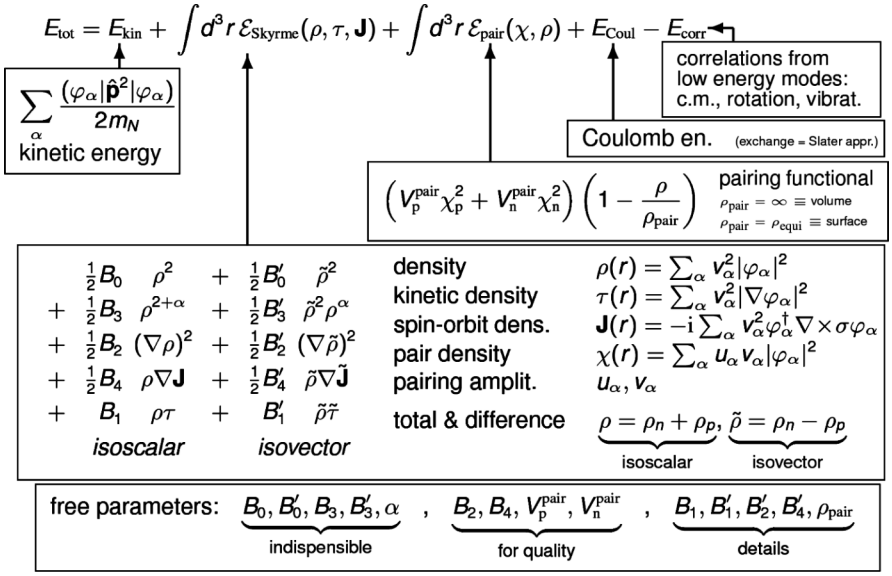

Fig. 1. Commented summary of the Skyrme energy functional, time-even couplings only

There is a great variety of strategies for the adjustment of the Skyrme parameters, for a summary see [4]. The conceptually most straightforward is a least squares fit to given set of experimental data [6]. The success relies on a proper selection of the fit data. Basic ground-state properties as binding energy, radii and surface thickness are, of course, first choice for observables. When the fit nuclei are concerned, one should carefully find out the best «mean field nuclei», i.e., those which are least influenced by ground-state correlations. A systematic investigation of correlations from low-energy quadrupole modes [17] led to the pool of fit nuclei as shown in Fig. 2. These are obviously chains of (spherical) semimagic nuclei. Part of them are already somewhat more affected by corre-

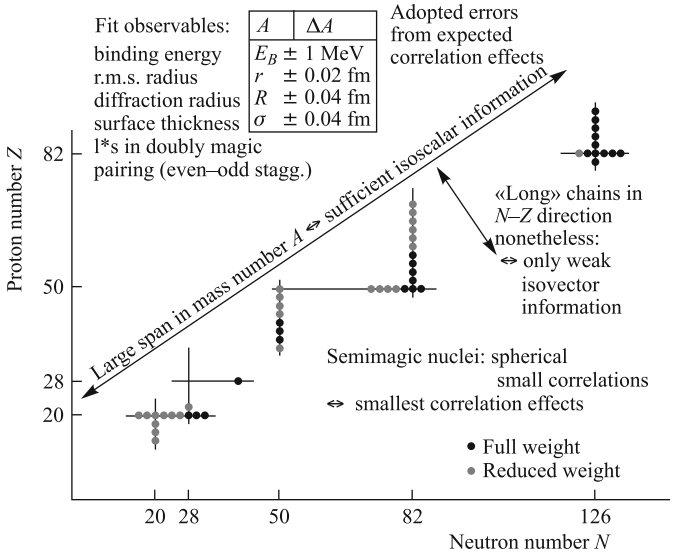

Fig. 2. Selection of fit nuclei and their adopted errors. Light grey dots indicate nuclei with somewhat larger correlation effects and less weight in the fit [3]

lations (light grey dots). These are included into the data pool, however with reduced weight. The quality measure is then composed as

$$\chi^2(\mathbf{p}) = \sum_{A\in\{\text{fit-data}\}} \frac{\left(A^{(\mathrm{SHF})}(\mathbf{p}) - A^{(\mathrm{exp})}\right)^2}{\Delta A^2}, \quad \mathbf{p} = (B_0, B_0', B_1, \ldots)\,, \qquad (1)$$

where A runs over all fit data, $\mathbf{p}$ stands for the set of free parameters, and ΔA is the adopted error on each data point. The adopted error produces a dimensionless contribution and regulates the relative weight of each entry. Their choice is also shown in Fig. 2 and the weight of the light grey nuclei is reduced by enhancing ΔA by a factor of two. The figure demonstrates immediately the problem with such a phenomenological adjustment. The chart of isotopes extends over a very broad pool of sizes which allows one to determine rather well the isoscalar terms in model 1. But the extension in isovector direction (orthogonal to system size) is extremely small which, in turn, means that isovector properties are only weakly determined, leaving space for further constraints (see the discussion of nuclear matter properties and the force SV-bas below). This explains the hierarchy of importance of parameters as quoted in Fig. 1.

As the input observables $A^{(\mathrm{SHF})}$, χ^2 is a function of the model parameters $\mathbf{p}$ and the aim is to find the absolute minimum. We perform minimization as

outlined in [8]. A detailed explanation of the fit data and subsequent fits is found in [3] and the name «SV-min» was given to the parameterization emerging from straightforward minimization to the data from finite nuclei.

The properties of a nuclear force are conveniently characterized by the nuclear matter properties (NMP) at equilibrium: binding energy E/A, density $\rho_{\rm equil}$, incompressibility K, effective mass m^*/m, symmetry energy $a_{\rm sym}$, and sum rule enhancement κ (= isovector effective mass). There is a known close relationship between these NMP and giant resonance properties. It is highly desirable to control the NMP together with finite nuclei data. To this end, we add optionally to fit data a commonly accepted set of NMP: $K = 234$ MeV, $m^*/m = 0.95$, $a_{\rm sym} = 30$ MeV, and $\kappa = 0.4$. A minimization with these NMP constraints yields a slightly different parameterization «SV-bas». The reproduction of finite nuclei data does not suffer much from the constraints, which indicates that these data leave some freedom for further aspects. It is to be mentioned that the predictions of SV-min for NMP deviate somewhat from the commonly believed values for $a_{\rm sym}$ and κ. Correlatively, the predictions for the giant dipole resonance (GDR) in ^{208}Pb do not match the data while SV-bas produces a correct GDR peak and, of course, better NMP. The difference between SV-min and SV-bas in connection with extrapolation errors helps to disentangle bulk properties from shell effects as we will see in the discussion of Fig. 3.

2. PREDICTIVE VALUE IN EXTRAPOLATIONS

The rules of χ^2 fitting also allow one to estimate the statistical errors for extrapolations to other observables B, not included in the fit data. It becomes

$$\Delta B = \sqrt{\sum_{i,j} \frac{\partial B}{\partial p_i} \left(\mathcal{C}^{-1}\right)_{ij} \frac{\partial B}{\partial p_j}}, \quad \mathcal{C}_{kl} = \frac{\partial^2 \chi}{\partial p_k \partial p_l}. \tag{2}$$

That is the allowed variation of the observable B within the ellipsoid of $\chi^2 - \chi^2_{\rm min} \leqslant 1$, i.e., for all χ^2 which stay at most one unit above the minimum. Figure 3 shows these extrapolation errors for binding energies and two-neutron separation energies along the chain of very neutron rich Sn isotopes, deep into the regime of the astrophysical r-process. The panel *a* for binding energies shows a systematic growth of the uncertainty when moving away from the fit regime. Freezing of NMP in SV-bas reduces the uncertainty by a factor of two, which shows that the uncertainty in an unrestricted fit as SV-min consists half out of uncertain bulk properties (= NMP) and half out of shell structure. The panel *b* for two-neutron separation energies behaves similarly, but the errors are much smaller than for the energies as such. Differences of energies probe the response properties and these are obviously much more robust. Note also the peak at

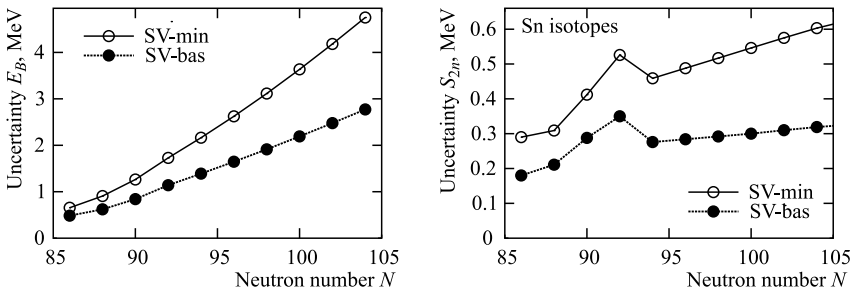

Fig. 3. The estimated uncertainty in the extrapolation of binding energies (*a*) and two-neutron separation energies (*b*) deep into the regime of neutron-rich Sn isotopes

neutron number $N = 92$. There is a small subshell closure which is particularly sensitive to shell structure. Accordingly the shell contribution has a peak while bulk properties (difference of the two curves) develop smoothly.

Statistical errors are easily evaluated within the method itself, as seen above. Much harder to control are the systematic errors which sneak in by possibly incomplete aspects of the given model, here the SHF functional (Fig. 1). A way to find them is to check the predictions of the model for other observables which were not included in the fit but for which experimental data are available. This is exemplified in Fig. 4 for the extrapolation to superheavy elements (SHE) for

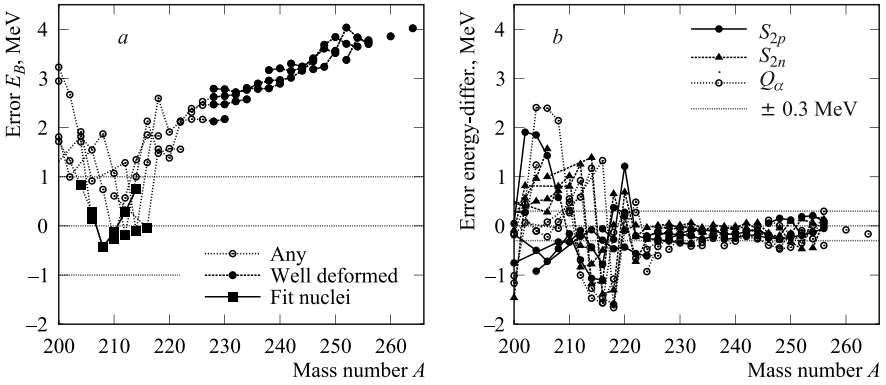

Fig. 4. Deviation between theory (parameterization SV-min) and experiment for the binding energies (*a*) and differences thereof (*b*) in the regime of (super-)heavy nuclei. The nuclei in the panel *a* are distinguished as: filled squares = fit nuclei, filled circles = well-deformed nuclei, open circles = vibrational soft nuclei. The panel *b* shows three sorts of energies differences: two-proton separation energy S_{2p} (filled circle), two-neutron separation energy S_{2n} (filled triangle), and Q_α value (open circle). Intended error limits are indicated by fine dotted lines, ± 1 MeV for binding energies and ± 0.3 MeV for their differences

the observables binding energies (panel *a*) and differences thereof (panel *b*). The figure shows that interpolation (results for nuclei $A < 210$) works well with errors remaining acceptably small and distributed on both sides of the zero line. But the extrapolation to binding energies of SHE (panel *a*) shows a significant trend to increasing underbinding. The same trend (often worse) is found for other Skyrme forces. On the other hand, all three types of energy differences (panel *b*) behave fairly well in the extrapolation. These observables are described reliably well, much better than the total binding energy. The reason for the dramatic mismatch of the total energy is still unknown and calls for further analysis.

The SHF approach does also allow one to compute excitation spectra by means of time-dependent SHF and its linearized version, often called random-phase approximation (RPA). A separable expansion thereof, called separable RPA (SRPA), provides a particularly efficient computational scheme [9] which allows systematic surveys even in deformed and heavy nuclei [10]. The dominant excitation modes are the isovector giant dipole resonances (GDR) which display a pronounced resonance peak [11]. The peak position is strongly related to the symmetry energy $a_{\rm sym}$ and sum rule enhancement κ [3]. There are many Skyrme parameterizations which provide an excellent description of GDR in heavy nuclei and these are precisely those which have reasonable values for $a_{\rm sym}$ and κ. It is interesting to check how these forces perform in the extrapolation to SHE. Figure 5 shows the trend of the GDR peak in the regime of SHE for the parameterization SLy6 [12] which was proven to perform reasonably well for stable heavy nuclei [9]. The SRPA results are compared with the empirical trend $E_{\rm BF} = (31.2A^{-1/3} + 20.6A^{-1/6})$ MeV which is a mix of surface and volume resonance modes [11]. This trend is basically continued and the SRPA results remain in the average comfortably close to the empirical prognosis. But the SRPA results show a strong isotopic effect, a positive curvature above the smooth, linear trend. Such an effect has not been seen for nuclei with lower Z. It is a new feature appearing in SHE. An explanation for this has yet to be worked out.

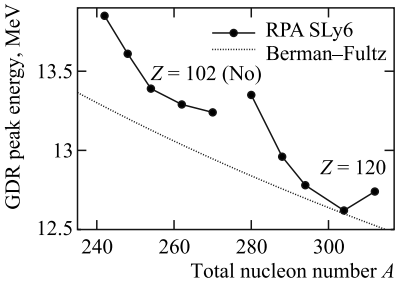

Fig. 5. Peak energies of the Giant Dipole Resonance (GDR) in two isotopic chains of superheavy elements. The trend deduced from the GDR in stable nuclei is indicated by a dotted line [11]

The mean-field description of nuclear fission is an extremely demanding task because all aspects of the effective nuclear interaction are probed, global parameters of the nuclear liquid drop as well as details of the shell structure. There are thus only few SHF studies of fission, see, e.g., [13–15]. We have re-

cently developed a fully self-consistent description of fission lifetimes [16] on the grounds of SHF. We summarize briefly the computational scheme [16]: The fission path is generated by quadrupole-constrained SHF whose energy expectation values yield a «raw» collective energy surface displaying a more or less large fission barrier. The collective mass and moments of inertia are computed by self-consistent cranking along the states of the path. Approximate projection onto zero angular momentum is performed and quantum corrections for the spurious vibrational zero-point energy are applied using the collective masses and widths. The collective ground-state energy is computed fully quantum mechanically [17]. The tunneling rate and the repetition rates are computed by the standard semiclassical formula (known as WKB) using the quantum-corrected potential energy and collective mass; the fission lifetime is finally composed of these two rates. All calculations are in axial symmetry. Figure 6 summarizes results on fission barriers and lifetimes for a few typical SHE and for a large variety of Skyrme parameterizations (SkM* [18], SkP [19], SkI3 [20], SLy6 [12] and SV-min [3]). The SHE represent two groups, one at the lower side and the other one with much heavier nuclei at the limits of present-day data. The span of predictions from the various Skyrme forces is huge in all cases in spite of the fact that all these parameterizations provide a high-level description of nuclear ground properties along the valley of stability. The variation of predictions is not necessarily a problem. On the contrary, one may use the fission properties as additional selection criterion for pinning down more precisely the most realistic parameterization. The problem appears when looking at the trend from the lighter side (Rf, Sg, Hs) to the heavier elements ($Z = 112$, 114). All parameterizations produce a wrong trend of the predictions from the lower to the upper region. One may argue that triaxiality, ignored here, could resolve the trend because triaxial deformation may lower some barriers selectively. But that is very unlikely in view of the experience that the triaxial barrier-lowering

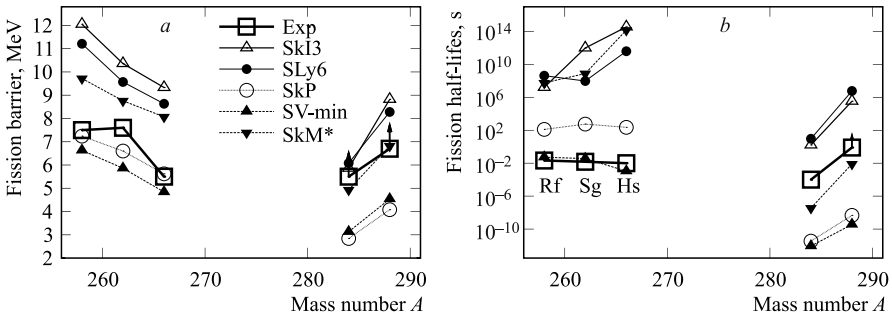

Fig. 6. Fission barriers (*a*) and lifetimes (*b*) for two chains of superheavy elements. Compared are results from a variety of Skyrme parameterizations with experimental data [21–24]

amounts typically to 0.5–2 MeV. This does not suffice to explain the mismatch in the trend as observed here. Again, the reasons for this failure have yet to be evaluated.

CONCLUSION

We have given a very brief overview over the present status of the Skyrme–Hartree–Fock (SHF) approach. We have discussed briefly the basic SHF energy functional and the phenomenological adjustment of its free parameters. One needs to sort out a set of observables for which a mean-field description is justified and which can be computed very efficiently. This limits the selection to spherical semimagic nuclei, ideally long isotopic and isotonic chains. The nature of the valley of stability allows one to determine isoscalar properties very well, while some uncertainties remain concerning isovector properties. This has immediate consequences for extrapolations from which we had discussed a few typical examples.

The least-squares techniques used for the adjustment imply a safe estimate for the statistical error in extrapolations. We have exemplified this for a chain of very neutron-rich Sn isotopes. The inherent uncertainty in isovector properties shows up as strong increase of uncertainty in total binding energies when departing from the known nuclei. On the other hand, differences of binding energies (two-neutron separation energy) remain much more reliable. An idea about the systematic error of the model is obtained by checking extrapolations for which experimental data are still available. This was done for various observables (energy, giant resonances, fission) in superheavy elements (SHE). Again it was confirmed that binding energies can be critical, while differences thereof are safe. Fission properties show a high sensitivity to the underlying Skyrme parameterization, but all existing parameterizations still fail to reproduce the trends of fission barriers and lifetimes from moderate SHE to the upper end of nuclei. Giant resonances in SHE are following basically known trends, but show a pronounced isotopic curvature not seen in less heavy nuclei.

The authors acknowledge support from the DFG (project RE-322/12-1), from the BMBF (contracts 06 DD 9052D and 06 ER 9063), and from the Heisenberg–Landau program (Germany–BLTP JINR).

REFERENCES

1. *Samyn M. et al.* // Nucl. Phys. A. 2002. V. 700. P. 142.
2. *Bertsch G. et al.* // Phys. Rev. C. 2005. V. 71. P. 054311.
3. *Klüpfel P. et al.* // Phys. Rev. C. 2009. V. 79. P. 034310.

4. *Bender M., Heenen P.-H., Reinhard P.-G.* // Rev. Mod. Rhys. 2003. V. 75. P. 121.
5. *Stone J.R., Reinhard P.-G.* // Prog. Part. Nucl. Phys. 2007. V. 58. P. 587.
6. *Friedrich J., Reinhard P.-G.* // Phys. Rev. C. 1986. V. 33. P. 355.
7. *Erler J., Klüpfel P., Reinhard P.-G.* // Eur. Phys. J. A. 2008. V. 37. P. 81.
8. *Bevington P. R.* Data Reduction and Error Analysis for the Physical Sciences. N. Y.: McGraw-Hill, 1969.
9. *Nesterenko V. O. et al.* // Phys. Rev. C. 2006. V. 74. P. 054306.
10. *Kleinig W. et al.* // Phys. Rev. C. 2008. V. 78. P. 044313.
11. *Berman B. L., Fultz S. C.* // Rev. Mod. Phys. 1975. V. 47. P. 713.
12. *Chabanat E. et al.* // Nucl. Phys. A. 1997. V. 627. P. 710.
13. *Berger J.-F. et al.* // Nucl. Phys. A. 2001. V. 685. P. 1c.
14. *Bürvenich T. et al.* // Phys. Rev. C. 2004. V. 69. P. 014307.
15. *Warda M. et al.* // Phys. Scr. T. 2006. V. 125. P. 226.
16. *Schindzielorz N.* // Intern. J. Mod. Phys. E. 2009. V. 18. P. 773.
17. *Klüpfel P. et al.* // Eur. Phys. J. A. 2008. V. 37. P. 343.
18. *Bartel J. et al.* // Nucl. Phys. A. 1982. V. 386. P. 79.
19. *Dobaczewski J., Flocard H., Treiner J.* // Nucl. Phys. A. 1984. V. 422. P. 103.
20. *Reinhard P.-G., Flocard H.* // Nucl. Phys. A. 1995. V. 584. P. 467.
21. *Audi G. et al.* // Nucl. Phys. A. 2003. V. 729. P. 3.
22. *Hofmann S. et al.* // Eur. Phys. J. A. 2001. V. 10. P. 5.
23. *Tandel S. K. et al.* // Phys. Rev. Lett. 2006. V. 97. P. 082502.
24. *Oganessian Yu. Ts. et al.* // Phys. Rev. C. 2006. V. 74. P. 044602.